Antiviral Research 99 (2013) 207–213

Contents lists available at SciVerse ScienceDirect

Antiviral Research

journal homepage: www.elsevier.com/locate/antiviral

A novel Ebola virus expressing luciferase allows for rapid and quantitative testing of antivirals

Thomas Hoenen [a,*], Allison Groseth [a], Julie Callison [a], Ayato Takada [b], Heinz Feldmann [a,*]

[a] Laboratory of Virology, Division of Intramural Research, National Institute of Allergy and Infectious Diseases, National Institutes of Health, Hamilton, MT, USA
[b] Research Center for Zoonosis Control, Hokkaido University, Japan

ARTICLE INFO

Article history:
Received 13 February 2013
Revised 29 May 2013
Accepted 30 May 2013
Available online 7 June 2013

Keywords:
Ebola virus
Luciferase
Firefly
Reverse genetics
Antiviral screening
High-throughput screening

ABSTRACT

Ebola virus (EBOV) causes a severe hemorrhagic fever with case fatality rates of up to 90%, for which no antiviral therapies are available. Antiviral screening is hampered by the fact that development of cytopathic effect, the easiest means to detect infection with wild-type EBOV, is relatively slow. To overcome this problem we generated a recombinant EBOV carrying a luciferase reporter. Using this virus we show that EBOV entry is rapid, with viral protein expression detectable within 2 h after infection. Further, luminescence-based assays were developed to allow highly sensitive titer determination within 48 h. As a proof-of-concept for its utility in antiviral screening we used this virus to assess neutralizing antibodies and siRNAs, with significantly faster screening times than currently available wild-type or recombinant viruses. The availability of this recombinant virus will allow for more rapid and quantitative evaluation of antivirals against EBOV, as well as the study of details of the EBOV life cycle.

Published by Elsevier B.V.

1. Introduction

Ebolaviruses are non-segmented negative sense RNA viruses in the family *Filoviridae*. Ebola virus (EBOV) causes a severe hemorrhagic fever in humans and non-human primates with case fatality rates in humans of up to 90% (Feldmann and Geisbert, 2011). Despite intensive research, there are no approved therapies available for treatment of Ebola hemorrhagic fever (Kondratowicz and Maury, 2012). One factor that has hindered the development of efficient therapies is the fact that wild-type EBOV is not very amenable to antiviral screening, which is at least in part due to the fact that development of cytopathic effect (CPE), which is the easiest way to detect infection, is relatively slow (Pegoraro et al., 2012).

Reverse genetics systems allow the generation of recombinant EBOVs (Hoenen et al., 2011), and have been used in the past to generate eGFP-expressing EBOVs (Ebihara et al., 2007; Towner et al., 2005), which allow much more rapid detection of infection *in vitro*. Using these viruses great progress has recently been made in developing high-content screening protocols for EBOV (Panchal et al., 2010; Pegoraro et al., 2012). However, high-content screening requires extensive and costly automated imaging equipment, and so far these protocols have relied on a multistep approach in which cells are first infected in a BSL4 laboratory for several days, and then fixed for several days in formalin before they are analyzed under BSL2 conditions (Panchal et al., 2012; Pegoraro et al., 2012).

Luminescent reporters provide a viable alternative to fluorescent reporters (Miraglia et al., 2011). They facilitate very sensitive cell-based reporter assays (Thorne et al., 2010), eliminate the problem of compound fluorescence (Simeonov et al., 2008), and have relatively modest instrumentation requirements. Therefore, as an alternative to the eGFP-expressing EBOV, we have developed a recombinant EBOV expressing Firefly luciferase (rgEBOV-luc2) as a reporter protein. We show that this virus allows extremely fast and sensitive detection of virus replication, with reporter activity first being detectable only 2 h post-infection. Further, this virus is amenable to assays in a 96-well format with excellent Z′-factors, can be used at very low infectious doses if required, has modest instrument requirements, and was successfully used to assess the effect of both antibodies and siRNAs directed against EBOV in a proof-of-concept study.

2. Materials and Methods

2.1. Cells

Vero E6 (African green monkey kidney, ATCC CRL-1586) (Earley and Johnson, 1988) and 293 (human embryonic kidney) cells were

Abbreviations: CPE, cytopathic effect; eGFP, enhanced green fluorescent protein; EBOV, Ebola virus; LBT assay, luminescence-based direct titration assay; luc2, codon-optimized Firefly luciferase; MOI, multiplicity of infection; RLU, relative light units; $TCID_{50}$, tissue culture infectious dose 50.

* Corresponding authors. Address: 903 S. 4th St., Hamilton, MT 59840, USA. Tel.: +1 406 375 7408 (T. Hoenen), tel.: +1 406 375 7410; fax: +1 406 375 9620 (H. Feldmann).

E-mail addresses: thomas.hoenen@nih.gov (T. Hoenen), feldmannh@mail.nih.gov (H. Feldmann).

0166-3542/$ - see front matter Published by Elsevier B.V.
http://dx.doi.org/10.1016/j.antiviral.2013.05.017

maintained in Dulbecco's modified Eagle medium (DMEM; Life Technologies) supplemented with 10% fetal bovine serum (FBS; Life Technologies), 2 mM L-glutamine (Q; Life Technologies), and 100 U/ml penicillin and 100 g/ml streptomycin (PS; Life Technologies) and grown at 37 °C with 5% CO_2.

2.2. Cloning and rescue of recombinant viruses

An additional transcriptional unit was inserted into a full-length clone plasmid (pAmp-rgEBOV) (Shabman et al., 2013) containing a cDNA copy of the EBOV genome (strain Mayinga, accession number AF086833.2) using standard cloning techniques (Fig. 1A). The open reading frame for a codon-optimized Firefly luciferase (luc2, Promega) or eGFP was then inserted into this additional transcriptional unit. Detailed cloning strategies can be found as Supplementary material. Rescue was performed as previously described (Hoenen et al., 2012). Briefly, Vero cells were transfected with 250 ng of full-length clone plasmid and expression plasmids for the EBOV proteins NP (125 ng), VP35 (125 ng), VP30 (75 ng) and L (1000 ng) as well as T7 polymerase (125 ng). 24 h post transfection the medium was exchanged, and 7 days post-transfection 1 ml of supernatant was passaged onto fresh Vero cells for growth of a virus stock. This stock was harvested upon development of CPE. The genomes of the rescued viruses were fully sequenced, with no unwanted mutations being identified. Stock titers were determined by CPE-based $TCID_{50}$ assay (see below).

2.3. Infections with recombinant viruses and luciferase activity measurements

Infections were performed as previously described (Hoenen et al., 2012). For time-course analysis of luciferase expression infections were performed in 6-well format on ice, and the supernatant was removed and cells scraped into 1 ml cold PBS at the indicated time-points after shifting the cells to 37 °C. 400 µl of these cells were spun down for 5 min at 1000*g* and 4 °C, and the pellet was resuspended in 200 µl 1x passive lysis buffer (Promega). Luciferase activity was measured in a GloMax-Multi Microplate Multimode Reader (Promega) 10 min after adding 100 µl lysate (equivalent to approximately 200,000 cells) to an equal amount of BrightGlo (Promega) in an opaque white 96-well plate.

For all other experiments, which were performed in 96-well format, luciferase activity was determined by removing the supernatant, adding 100 µl Glo lysis buffer (Promega) to the cells, incubating them for 10 min at room temperature for passive lysis, and then measuring the luciferase activity in 40 µl of lysate (equivalent to approximately 8000 cells) as described above.

Experiments with recombinant EBOV were approved by the Institutional Biosafety Committee (IBC) and performed in BSL4 containment at the Rocky Mountain Laboratories (RML), Division of Intramural Research (DIR), National Institute of Allergy and Infectious Diseases (NIAID), National Institutes of Health (NIH), following standard operating procedures.

2.4. $TCID_{50}$, luminescence-based $TCID_{50}$ and LBT assays

$TCID_{50}$ assays were performed by infecting Vero cells in 96-well format with a tenfold dilution series of samples, infecting 4 wells per sample and dilution step (for stock titrations 8 wells per sample and dilution step were infected). CPE-based $TCID_{50}$ assays were read after 18 days, to ensure a definitive distinction between infected and uninfected wells even at higher dilutions. Luminescence-based $TCID_{50}$ assays were read by measuring luciferase activity at the indicated time points, as described above. Wells were deemed positive when reporter activity was at least 1 $\log_{10}$ higher than in uninfected control samples and not more than 2 $\log_{10}$ lower than directly neighboring wells, to compensate for cross-talk between different dilution steps. To further eliminate the possibility of crosstalk between different samples, at least one column was left empty between these samples when measuring luciferase activity. Titers were calculated using the Spearman–Kaerber method (Wulff et al., 2012).

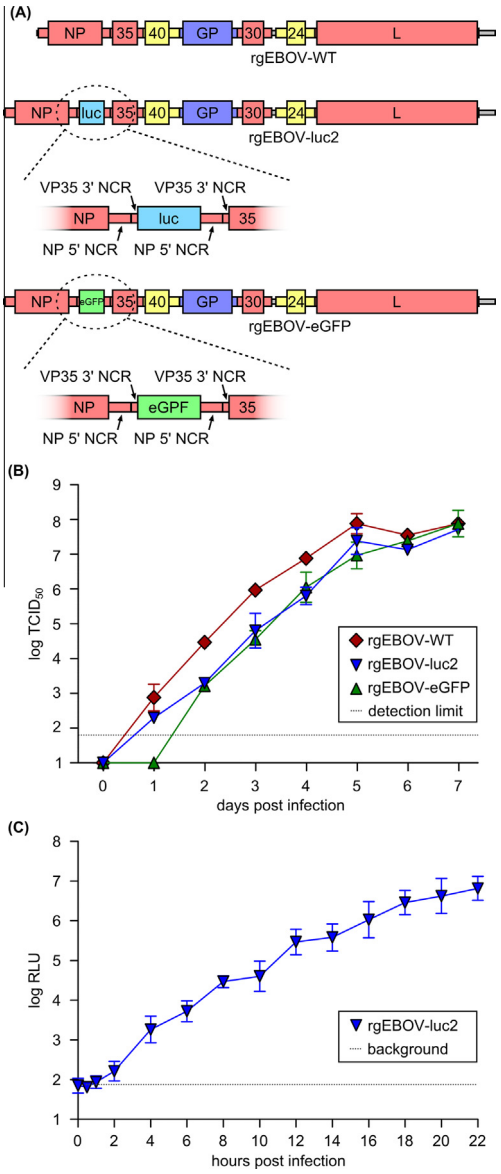

Fig. 1. Design and basic characterization of rgEBOV-luc2. (A) Genome structure of recombinant viruses. The genome structures of rgEBOV-WT, rgEBOV-luc2 and rgEBOV-eGFP are shown. Coding regions are depicted as broad bars together with their respective gene names (VP35, VP40, VP30 and VP24 are abbreviated as 35, 40, 30 and 24, respectively). Non-coding regions (NCR) are depicted as narrow bars using the same color scheme as the corresponding coding regions (red: nucleocapsid protein genes, yellow: matrix protein genes; dark blue: glycoprotein gene). Untranscribed regions are depicted as grey bars. For rgEBOV-luc2 and rgEBOV-eGFP the inserted genes are shown in light blue or green, respectively, with the blowups showing the NCRs surrounding the coding regions. (B) Growth kinetics of rgEBOV-luc2. Vero cells were infected with rgZEBOV-WT, rgZEBOV-luc2 and rgEBOV-eGFP at an MOI of 0.1. Supernatant titers were determined daily for 7 days by $TCID_{50}$. Mean and standard deviation from 3 independent experiments are shown. (C) Time-course analysis of reporter gene expression. Vero cells were infected for 1 h on ice with rgZEBOV-WT at an MOI of 0.5. The inoculum was removed, and cells were shifted to 37 °C. Reporter activity in cell lysates was measured at the indicated time points after infection. The dashed line indicates the background noise of the luminometer (background). Mean and standard deviation from 3 independent experiments are shown. (For interpretation of the references to colour in this figure legend, the reader is referred to the web version of this article.)

For the luminescence-based direct titration (LBT) assay, 50 µl of undiluted and 1:1000 diluted unknown samples were used to infect Vero cells in 96-well format in a total volume of 100 µl, along with known virus standards (5×10^5, 5×10^4, 5×10^3, 5×10^2 $TCID_{50}$/ml). All infections were done in triplicate. 48 h post-infection, luciferase activity was measured as described above, and a linear regression curve based on the virus standard samples was used to calculate the titer of the unknown samples based on their luciferase activity.

2.5. Testing of neutralizing antibodies and siRNAs

For testing of neutralizing antibodies, 100 $TCID_{50}$ of rgEBOV-luc2 were incubated with the previously characterized neutralizing antibodies 133/3.16 or 226/8.1 or the non-neutralizing antibody 42/3.7 (Takada et al., 2003) at the indicated concentrations in a total volume of 100 µl in a 96-well plate. After 1 h, 2×10^4 Vero cells in 100 µl were added to each well. After 2 days luciferase activity was determined as described above.

For testing of siRNAs, 293 cells at a confluency of ~50% were transfected with the indicated amount of L-specific Dicer substrate siRNA (DsiRNA) duplex (5′-rGrArUrCrArArUrUrUrArUrArUrArCrArGrCrUrUrCrGrUrArCrArA-3′, 5′-rGrUrArCrGrArArGrCrUrGrUrArUrArUrArArArUrUrGrArTrC-3′; Integrated DNA Technologies) or control DsiRNAs (NC1 and DS Scrambled Neg, Integrated DNA Technologies). To this end, the DsiRNA was diluted in 5 µl Opti-MEM (Invitrogen; all amounts are per well), and 0.3 µl Lipofectamine 2000 (Invitrogen) in 5 µl Opti-MEM was added to the diluted DsiRNA. After 5 min incubation, the complexes were diluted 1:5 in DMEM without FBS, and 50 µl diluted complex was added to each well, for a final volume of 100 µl per well. 24 h later, 100 $TCID_{50}$ rgEBOV-luc2 in 50 µl medium were added to the cells. 2 days post-infection luciferase activity was determined as described above.

2.6. Statistical analysis

Statistical analysis was performed using the Prism 5 software (GraphPad Software). Z′-factors (separation band/dynamic range of the assay: $[(\mu_{c+} - 3\sigma_{c+}) - (\mu_{c-} - 3\sigma_{c-})]/(\mu_{c+} - \mu_c)$, with μ being mean and σ being the standard deviation of the positive control c+ or the negative control c− of the assay) were calculated as previously described (Zhang et al., 1999).

3. Results and discussion

3.1. Generation and characterization of a recombinant EBOV expressing Firefly luciferase

In order to generate a recombinant EBOV that allows rapid detection of infection, we inserted a Firefly luciferase gene codon optimized for expression in mammalian cells into the EBOV genome between the genes for NP and VP35 (Fig. 1A), similar to published recombinant EBOVs expressing eGFP (Ebihara et al., 2007; Towner et al., 2005). This virus (rgEBOV-luc2) was readily rescued, and showed only a slight attenuation in Vero cells, when compared to a recombinant wild-type virus (rgEBOV-WT), and reached the same endpoint titers (Fig. 1B). Also, its growth was virtually identical to a recombinant EBOV expressing eGFP (rgEBOV-eGFP) that was rescued in parallel (Fig. 1B). This is consistent with previous observations that insertion of an additional gene at this position has no or only a slight impact on growth kinetics *in vitro*, depending on the cell line used (Ebihara et al., 2007; Towner et al., 2005).

In order to further characterize rgEBOV-luc2, we infected Vero cells with this virus, and measured luciferase activity at 0, 0.5, 1, 2 h post-infection and then every 2 h until 22 h post-infection (Fig. 1C). It has to be noted that in this experiment, which was performed in a 6-well format, we measured the luciferase signal in approximately 200,000 cells, whereas in all other experiments, which were performed in 96-well format, we measured the luciferase signal in approximately 8000 cells. Mock-infected cell lysates and lysates from cells infected with rgEBOV-WT (Figure S1) as well as the first three time-points (0, 0.5 and 1 h post-infection) did not yield any signal significantly above the background noise of the

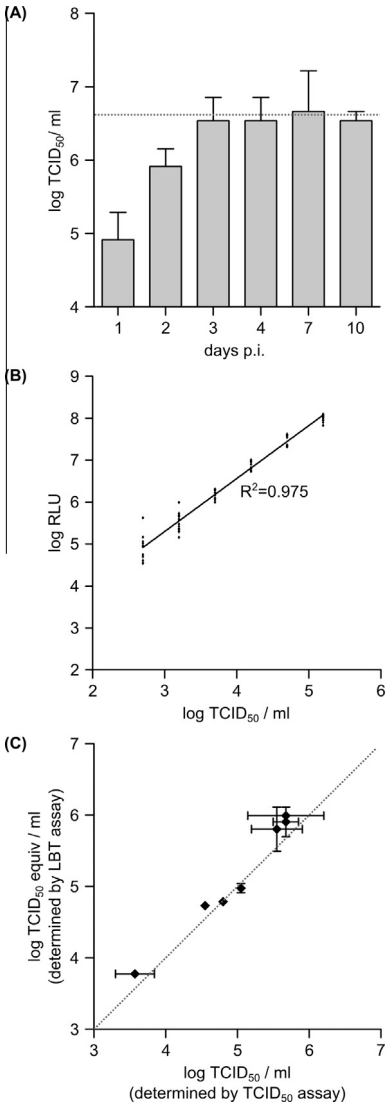

Fig. 2. Titration assays for rgEBOV-luc2. (A) Luminescence-based $TCID_{50}$ assay. $TCID_{50}$ assays using luminescence as a read-out were performed on an rgZEBOV-luc2 virus stock with a known concentration ($10^{6.6}$ $TCID_{50}$/ml; indicated by the dotted line). At the indicated time points post-infection the $TCID_{50}$ assay was evaluated, and the input titer calculated. Mean and standard deviation of 4 biological replicates from 2 independent experiments are shown. (B) Linear relationship between infectious dose and luciferase activity. Vero cells were infected with a dilution series of rgZEBOV-luc2 of known concentration. 2 days post-infection luciferase activity in relative light units (RLU) was measured. 14 biological replicates per dilution from 2 independent experiments, as well as a linear regression curve and the coefficient of determination (R^2) of that curve, are shown. (C) Comparison of luminescence-based direct titration assay and $TCID_{50}$ assay. Experimental samples containing varying amounts of rgZEBOV-luc2 were titrated using a luminescence-based $TCID_{50}$ assay or a luminescence-based direct titration (LBT) assay, and for each sample the titer, as determined by $TCID_{50}$ assay was plotted in relation to the titer determined by LBT assay. The dotted line indicates identical $TCID_{50}$ vs. LBT titers. Shown are mean and standard deviation of three replicates of the respective titration assays.

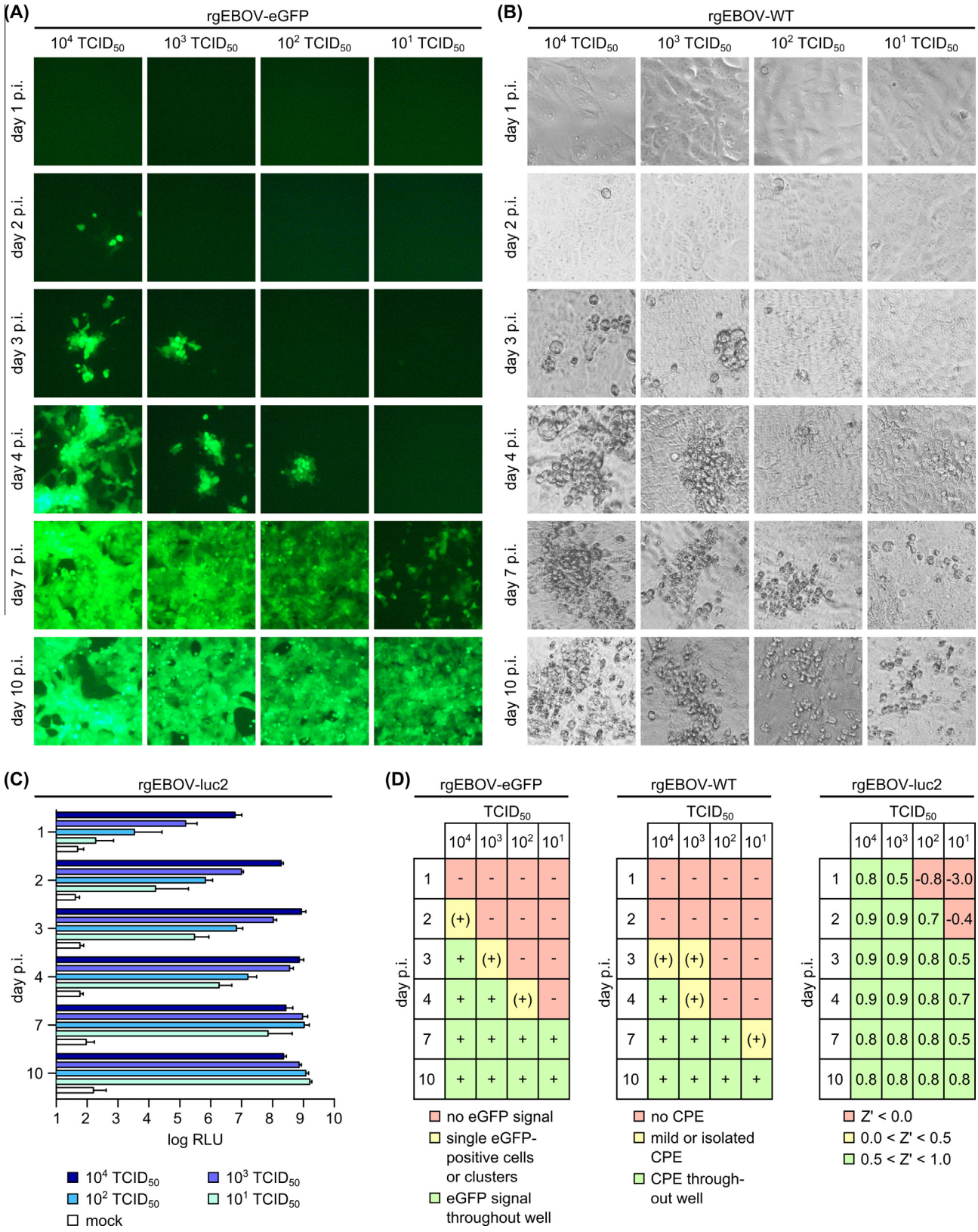

Fig. 3. Comparison of rgZEBOV-GFP, rgZEBOV-luc2 and rgZEBOV-WT. (A) Reporter activity generated by infection with rgZEBOV-eGFP. Vero cells were infected with the indicated doses of rgZEBOV-eGPF. eGFP-signals were visualized at the indicated times post-infection using fluorescence microscopy. (B) CPE generated by infection with rgZEBOV-WT. Vero cells were infected with the indicated doses of rgZEBOV-WT. CPE was visualized at the indicated times post-infection using phase contrast microscopy. (C) Reporter activity generated by infection with rgZEBOV-luc2. Vero cells were infected with the indicated doses of rgZEBOV-luc2, and luciferase activity was measured at the indicated times post-infection. Mean and standard deviation of 16 biological replicates from 2 independent experiments are shown. (D) Comparison of different viruses. For rgZEBOV-eGPF and rgZEBOV-WT the extent of eGFP-signal or cytopathic effect (CPE) for each infectious dose and time after infection is shown. For rgZEBOV-luc2, the Z′-factor (separation band/dynamic range) for each infectious dose and time-point after infection is shown.

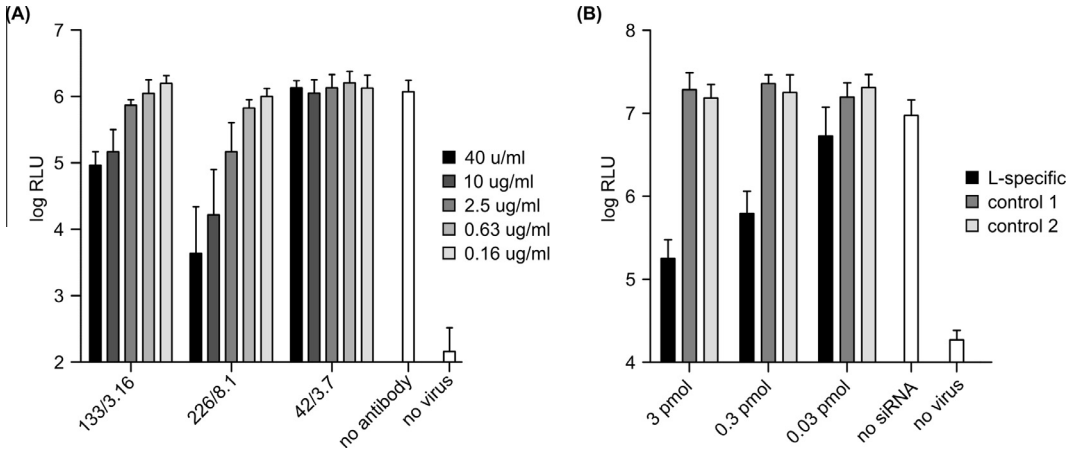

Fig. 4. rgEBOV-luc2 as tool for antiviral testing. (A) Testing of neutralizing antibodies. Vero cells were infected with 100 $TCID_{50}$ rgZEBOV-luc2 (MOI 0.005), which had been preincubated for 1 h with neutralizing (133/3.16 and 226/8.1) or non-neutralizing (42/3.7) antibodies at the indicated concentrations. 2 days post-infection luciferase activity in relative light units (RLU) was measured. Mean and standard deviation of 6 biological replicates from 2 independent experiments are shown. (B) Testing of DsiRNAs. 293 cells were transfected with the indicated amounts of L-specific or negative control DsiRNAs (control 1: NC1; control 2: Ds Scrambled Neg). 24 h post-transfection, cells were infected with 100 $TCID_{50}$ rgZEBOV-luc2 (MOI 0.005). 2 days post-infection luciferase activity in relative light units (RLU) was measured. Mean and standard deviation of 8 biological replicates from 2 independent experiments are shown.

luminometer, which for the luminometer used was $\sim 10^2$ RLU (at 1 h post-infection we observed a signal that was 21% above the signal of mock-infected cells; however, this increase was not statistically significant (Student's *t*-test: $p = 0.07$)). In contrast, at 2 h post-infection we detected a significant increase in reporter activity ($p = 0.03$), indicating that uptake of virus and initiation of viral gene expression require less than 2 h. Using qRT-PCR we have previously shown an increase in viral mRNA levels as early as 4 h post-infection (Hoenen et al., 2012). The fact that we could detect viral gene expression even earlier using rgEBOV-luc2 highlights the sensitivity of the luciferase reporter.

3.2. Development of luminescence-based TCID50 and LBT assays

As cells infected with rgEBOV-luc2 showed a very rapid increase in reporter signal, we decided to assess the possibility of using luminescence as a read-out in a $TCID_{50}$ assay. This would provide an advantage since CPE-based $TCID_{50}$ assays require a relatively long incubation to allow a clear distinction between infected and uninfected wells, particularly at higher dilutions. To this end, we performed $TCID_{50}$ assays on a virus stock with known concentration, measured luciferase activity after 1, 2, 3, 4, 7 and 10 days to determine infected vs. uninfected wells, and then calculated a $TCID_{50}$ titer based on these data (Fig. 2A). While at 1 and 2 days after infection the calculated titer did not concur with the actual titer, after 3 days and at all later time points the luminescence-based $TCID_{50}$ matched the actual titer as previously determined by CPE-based $TCID_{50}$ analysis, indicating that this assay reliably allows rapid titration of rgEBOV-luc2 within 3 days, and is able to detect single infectious particles (as determined by conventional $TCID_{50}$) with the same sensitivity as conventional $TCID_{50}$ assays.

When analyzing the data from the $TCID_{50}$ assay, we observed that the reporter signal declined about 1 $\log_{10}$ for each of the 10-fold dilution steps (data not shown), which lead us to explore the possibility of a linear relationship between reporter activity and input virus titer. To this end, we performed a 0.5 $\log_{10}$ dilution series of our virus stock, and determined reporter activity for each sample 2 days post-infection (Fig. 2B). Our data show that there is a clear linear relation between the input titer and luciferase activity in the range between $10^{2.7}$ $TCID_{50}$/ml and $10^{5.2}$ $TCID_{50}$/ml. At higher titers we no longer observed an equivalent increase in reporter activity, most likely due to the fact that these signals exceeded the linear dynamic range of the luminometer, whereas at lower titers we observed occasional samples that showed only background activity, suggesting that at these low concentration stochastic effects (i.e. an increasing probability that a sample of a highly diluted virus contains no infectious particles) start to significantly influence the outcome of the assay. Based on these findings, we developed a luminescence-based direct titration assay, in which the luminescence of an unknown sample is compared to a known standard dilution series. In order to increase the linear range of this assay, we measured both undiluted and 1000-fold diluted samples, to circumvent the fact that higher titers exceeded the linear dynamic range of the luminometer. To evaluate this assay, unknown samples were titered both using luminescence-based $TCID_{50}$ assays and LBT assays, and both titration methods showed good concurrence (Fig. 2C), indicating that the LTB assay can be used to accurately titer rgEBOV-luc2 samples within 2 days.

3.3. Comparison of rgEBOV-luc2, rgEBOV-eGFP and rgEBOV-WT

One obvious application for the rgEBOV-luc2 virus is in the screening for antivirals. In order to determine the minimum turnaround time for a screening assay, we infected Vero cells in 96-well format with different virus doses (10^4, 10^3, 10^2 and 10^1 $TCID_{50}$ per well, equivalent to MOIs of 0.5, 0.05, 0.005 and 0.0005, respectively), and measured luciferase activity after 1, 2, 3, 4, 7 and 10 days. We did not test a lower infectious doses of 10^0 $TCID_{50}$ per well, since at such a low dose stochastic effects would start to play an unacceptably large role, resulting in only 50% of the tested wells being infected. For comparison, infections were also performed using rgEBOV-eGFP, using eGFP fluorescence as a read-out, and rgEBOV-WT, using CPE as a read-out. For rgEBOV-eGFP, the first isolated eGFP-positive cells appeared after 2 days in wells receiving the highest dose, and after 4 days using 10^2 $TCID_{50}$ (Fig. 3A). However, the eGFP-positive cells were initially very rare and locating them required extensive scanning of the well. A robust eGFP-signal throughout most of the well became apparent after 3 to 4 days using higher doses (10^4 and 10^3 $TCID_{50}$), but only after 7 days at lower doses (10^2 $TCID_{50}$). Similar results were obtained using rgEBOV-WT, with mild isolated CPE becoming apparent between 3 and 7 days post-infection, depending on the infectious dose, and clear CPE throughout the well being visible at day 4 post-infection using the highest dose, and 7 to 10 days

post-infection for the other doses (Fig. 3B). In contrast, an increase in reporter activity was already detected using rgEBOV-luc2 for all infectious doses at day 1 post-infection (Fig. 3C). When determining the Z′-factor (Zhang et al., 1999), infectious doses of 10^3 $TCID_{50}$ or higher yielded Z′-factors of >= 0.5 already at day 1, indicating a very robust assay, whereas the lower doses of 10^2 and 10^1 $TCID_{50}$ yielded a Z′-factor of >= 0.5 at days 2 and 3 post-infection, respectively (Fig. 3D). When comparing this to the results obtained with rgEBOV-eGFP and rgEBOV-WT, it becomes apparent that rgEBOV-luc2 allows much quicker turnaround times for screening assays, and represents an extremely robust assay even at low infectious doses (Fig. 3D). For comparison, all drug-screening efforts with eGFP-expressing EBOV have thus far used high infectious doses (MOI = 5), with readout 2 days post-infection (Panchal et al., 2010, 2012).

3.4. Use of rgEBOV-luc2 as antiviral screening tool

As a proof-of-concept that rgEBOV-luc2 is feasible for use as an antiviral screening tool, we assessed the effect of two well-characterized neutralizing antibodies as well as the effect of a DsiRNA directed against the viral polymerase L. For testing of the neutralizing antibodies, 100 $TCID_{50}$ (equivalent to an MOI of 0.005) of rgEBOV-luc2 were preincubated with the previously characterized neutralizing antibodies 133/3.16 and 226/8.1 or the non-neutralizing antibody 42/.37, and then used to infect Vero cells. After two days, reporter activity was measured. As expected, there was a clear drop in reporter activity for both neutralizing antibodies, with 226/8.1 showing a 2.6 $\log_{10}$ reduction at the highest antibody concentration, and 133/3.16 showing a 1.2 $\log_{10}$ reduction at this concentration (Fig. 4A). In previous studies 226/8.1 showed a higher neutralizing activity than 133/3.16 (Takada et al., 2003), clearly corresponding to our results. For testing of the DsiRNA, 293 cells were pretransfected with a DsiRNA directed against L (targeting the same region as the siRNA EK1, that has been successfully used to protect both guinea pigs and NHPs against lethal EBOV challenge (Geisbert et al., 2006, 2010)) or control DsiRNAs, and then infected with 100 $TCID_{50}$ (equivalent to an MOI of 0.005) of rgEBOV-luc2. After two days, reporter activity was measured, and as expected we observed a clear drop in reporter activity of about 2 $\log_{10}$ at the highest amount of DsiRNA used, and smaller reductions of reporter activity at lower amounts of DsiRNA (Fig. 4B). No effects of the control DsiRNAs were observed, indicating that the reduction in reporter activity was due to a sequence specific effect of the DsiRNA on virus replication.

3.5. Conclusions

Antiviral screening of EBOV poses unique challenges. While reporter-expressing recombinant EBOVs have enabled rapid detection of infection, the need for a BSL4 laboratory when working with live virus remains, making fully automated high-throughput screenings for these viruses challenging. However, screening of libraries containing several thousand compounds in a 96-well format is feasible, as was recently demonstrated (Panchal et al., 2012), and rgEBOV-luc2 is highly amenable to be used in such a screen. rgEBOV-luc2 also has several advantages over eGFP-expressing EBOVs, including its ease of use (no requirement for removal of samples from BSL4, very little labor intensive), low equipment costs and the ability to use either a much lower infectious dose, or alternatively the much faster readout times when using higher infectious doses. These faster readout times, in addition to obvious practical advantages, also mean that compounds with a low stability in culture medium can be more reliably screened. However, too short readout times also have to be avoided, since otherwise the virus does not have time to complete a full life cycle, which would results in inhibitors of late stages of the virus life cycle (e.g. budding inhibitors) not being recognized in the screen. In contrast, high-content screening, which so far is the most extensively used screening approach that has been performed with EBOV-GFP, requires extensive and costly automated imaging equipment. Until now this kind of screening has relied on a multistep approach in which cells are first infected in a BSL4 laboratory for several days, and then fixed for several days in formalin before they are analyzed under BSL2 conditions (of course we cannot exclude the possibility that despite the very complex technology high-content imaging will in future become available under BSL4 conditions). However, high-content imaging with GFP-expressing EBOVs also has advantages over a simple reporter-based screening assay with luciferase-expressing viruses. Particularly, it allows one to assess a number of parameters such as cell viability and GFP expression at the same time. Further, measurement of GFP reporter activity can be done multiple times on the same sample. In contrast, measuring reporter activity of rgEBOV-luc2 represents an end-point assay, since cells have to be lysed prior to measurement. Another alternative that has only very recently been explored is the use of rgEBOV-GFP for screening purposes in the absence of high-content imaging, just relying on overall GFP expression in a well (Filone et al., 2013). Such an approach offers low equipment costs, comparable to luciferase-based assays, and is even less labor intensive, since no reagents have to be added for measurement. However, our data clearly show that under such conditions GFP-expressing viruses provide significantly lower sensitivity than luciferase-expressing viruses, and require much longer assay times. As a consequence, the only study that has employed this approach so far used a high infectious dose (MOI of 1) and readout times of 5 days after infection for EC50 determination, and 3 days after infection for direct visualization of GFP expression (Filone et al., 2013), which corresponds well to our own results (Fig. 3A).

Overall, both reporters offer advantages and disadvantages in relation to each other, and the choice of which virus to use will depend on the nature and requirements of the screening to be performed. Nevertheless, while further validation studies in a high-throughput setting are necessary, the present proof-of-concept study already suggests that rgEBOV-luc2 represents an interesting alternative to eGFP-expressing EBOVs for antiviral drug-screening.

Acknowledgement

This research was supported by the Intramural Research Program of the NIH, NIAID.

Appendix A. Supplementary data

Supplementary data associated with this article can be found, in the online version, at http://dx.doi.org/10.1016/j.antiviral.2013.05.017.

References

Earley, E.M., Johnson, K.M., 1988. The lineage of Vero, Vero 76 and its clone C1008 in the United States. In: Simizu, B., Terasima, T. (Eds.), Vero Cells-Origin, Properties and Biomedical Applications. Soft Science Publications, Tokyo, pp. 26–29.

Ebihara, H., Theriault, S., Neumann, G., Alimonti, J.B., Geisbert, J.B., Hensley, L.E., Groseth, A., Jones, S.M., Geisbert, T.W., Kawaoka, Y., Feldmann, H., 2007. In vitro and in vivo characterization of recombinant Ebola viruses expressing enhanced green fluorescent protein. J. Infect. Dis. 196 (Suppl. 2), S313–322.

Feldmann, H., Geisbert, T.W., 2011. Ebola haemorrhagic fever. Lancet 377, 849–862.

Filone, C.M., Hodges, E.N., Honeyman, B., Bushkin, G.G., Boyd, K., Platt, A., Ni, F., Strom, K., Hensley, L., Snyder, J.K., Connor, J.H., 2013. Identification of a broad-spectrum inhibitor of viral RNA synthesis: validation of a prototype virus-based approach. Chem. Biol. 20, 424–433.

Geisbert, T.W., Hensley, L.E., Kagan, E., Yu, E.Z., Geisbert, J.B., Daddario-DiCaprio, K., Fritz, E.A., Jahrling, P.B., McClintock, K., Phelps, J.R., Lee, A.C., Judge, A., Jeffs, L.B.,

MacLachlan, . Postexposure protection of guinea pigs against a lethal ebola virus challenge is conferred by RNA interference. J. Infect. Dis. 193, 1650–1657.
Geisbert, T.W., Lee, A.C., Robbins, M., Geisbert, J.B., Honko, A.N., Sood, V., Johnson, J.C., de Jong, S., Tavakoli, I., Judge, A., Hensley, L.E., Maclachlan, I., 2010. Postexposure protection of non-human primates against a lethal Ebola virus challenge with RNA interference: a proof-of-concept study. Lancet 375, 1896–1905.
Hoenen, T., Groseth, A., de Kok-Mercado, F., Kuhn, J.H., Wahl-Jensen, V., 2011. Minigenomes, transcription and replication competent virus-like particles and beyond: reverse genetics systems for filoviruses and other negative stranded hemorrhagic fever viruses. Antiviral Res. 91, 195–208.
Hoenen, T., Shabman, R.S., Groseth, A., Herwig, A., Weber, M., Schudt, G., Dolnik, O., Basler, C.F., Becker, S., Feldmann, H., 2012. Inclusion bodies are a site of ebolavirus replication. J. Virol. 86, 11779–11788.
Kondratowicz, A.S., Maury, W.J., 2012. Ebolavirus: a brief review of novel therapeutic targets. Future Microbiol. 7, 1–4.
Miraglia, L.J., King, F.J., Damoiseaux, R., 2011. Seeing the light: luminescent reporter gene assays. Comb. Chem. High Throughput Screen. 14, 648–657.
Panchal, R.G., Kota, K.P., Spurgers, K.B., Ruthel, G., Tran, J.P., Boltz, R.C., Bavari, S., 2010. Development of high-content imaging assays for lethal viral pathogens. J. Biomol. Screen. 15, 755–765.
Panchal, R.G., Reid, S.P., Tran, J.P., Bergeron, A.A., Wells, J., Kota, K.P., Aman, J., Bavari, S., 2012. Identification of an antioxidant small-molecule with broad-spectrum antiviral activity. Antiviral Res. 93, 23–29.
Pegoraro, G., Bavari, S., Panchal, R.G., 2012. Shedding light on filovirus infection with high-content imaging. Viruses 4, 1354–1371.
Shabman, R.S., Hoenen, T., Groseth, A., Jabado, O., Binning, J.M., Amarasinghe, G.K., Feldmann, H., Basler, C.F., 2013. An upstream open reading frame modulates Ebola virus polymerase translation and virus replication. PLoS Pathog. 9, e1003147.
Simeonov, A., Jadhav, A., Thomas, C.J., Wang, Y., Huang, R., Southall, N.T., Shinn, P., Smith, J., Austin, C.P., Auld, D.S., Inglese, J., 2008. Fluorescence spectroscopic profiling of compound libraries. J. Med. Chem. 51, 2363–2371.
Takada, A., Feldmann, H., Stroeher, U., Bray, M., Watanabe, S., Ito, H., McGregor, M., Kawaoka, Y., 2003. Identification of protective epitopes on ebola virus glycoprotein at the single amino acid level by using recombinant vesicular stomatitis viruses. J. Virol. 77, 1069–1074.
Thorne, N., Inglese, J., Auld, D.S., 2010. Illuminating insights into firefly luciferase and other bioluminescent reporters used in chemical biology. Chem. Biol. 17, 646–657.
Towner, J.S., Paragas, J., Dover, J.E., Gupta, M., Goldsmith, C.S., Huggins, J.W., Nichol, S.T., 2005. Generation of eGFP expressing recombinant Zaire ebolavirus for analysis of early pathogenesis events and high-throughput antiviral drug screening. Virology 332, 20–27.
Wulff, N.H., Tzatzaris, M., Young, P.J., 2012. Monte Carlo simulation of the Spearman-Kaerber TCID50. J. Clin. Bioinform. 2, 5.
Zhang, J.H., Chung, T.D., Oldenburg, K.R., 1999. A simple statistical parameter for use in evaluation and validation of high throughput screening assays. J. Biomol. Screen. 4, 67–73.